DELSY project: status and development†

N. Balalykin,[a] P. Beloshitsky,[a] V. Bykovsky,[a] V. Kobets,[a] V. Kolobanov,[b] G. Kulipanov,[c] E. Levichev,[c] V. Mikhaylin,[b] I. Meshkov,[a]* N. Mezentsev,[c] N. Morozov,[a] I. Seleznev,[a] G. Sidorov,[a] A. Skrinsky,[c] G. Shirkov,[a] E. Syresin,[a] I. Titkova[a] and M. Yurkov[a]

[a]Joint Institute for Nuclear Research, 141980 Dubna, Moscow Region, Russia, [b]Moscow State University, Moscow 119992, Russia, and [c]Budker Institute of Nuclear Physics, 630090 Novosibirsk, Russia. E-mail: meshkov@nusun.jinr.ru

The DELSY (Dubna Electron Synchrotron) project is under development at the Joint Institute for Nuclear Research [Arkhipov *et al.* (2001). *Nucl. Instrum. Methods*, A**467**, 57–62; Arkhipov *et al.* (2001). *Nucl. Instrum. Methods*, A**470**, 1–6; Titkova *et al.* (2000). *Proceedings of the Seventh European Particle Accelerator Conference*, pp. 702–704]. It is based on an acceleration facility donated to the Joint Institute for Nuclear Research by the Institute for Nuclear and High Energy Physics (NIKHEF, Amsterdam). The NIKHEF accelerator facility consists of the linear electron accelerator MEA, which has an electron energy of 700 MeV, and the electron storage ring AmPS, with a maximum energy of 900 MeV and a beam current of 200 mA. There are three phases to the construction of the DELSY facility. Phase I will be accomplished with the construction of a complex of free-electron lasers covering continuously the spectrum from the far infrared down to the ultraviolet (~150 nm). Phase II will be accomplished with the commissioning of the storage ring DELSY. Complete commissioning of the DELSY project will take place after finishing Phase III, the construction of an X-ray free-electron laser. This phase is considered as the ultimate goal of the project; it is currently under development and is not described in this paper.

Keywords: storage rings; insertion devices.

1. Phase I: complex of free-electron lasers

The linear accelerator MEA will be used for two purposes: electron injection into the DELSY ring (Phase II) and pumping of the free-electron lasers. The latter cover a wide spectrum from the far infrared down to the ultraviolet (Table 1).

The key element of a free-electron laser (FEL) is an undulator (or wiggler) which forces the electrons to move along a curved periodical trajectory. There are two popular undulator configurations: helical and planar. The technology of the construction of the planar undulators is much better developed, and planar undulators are used in almost all operating FELs. In the DELSY FELs we plan to use planar undulators (Table 2), and will consider application of other kinds in the future.

The driving beam for a FEL has to have the peak current in the bunch as large as possible (Saldin *et al.*, 2000). Indeed, the micropulse separation can be much larger than the RF oscillation period (~0.3 ns in our case). Its upper limit is given by the round-trip time of the optical pulse in the FEL optical cavity (50 ns for the DELSY parameters). The beam accelerated in the DELSY linac will have parameters (Table 3) sufficient for driving the FEL oscillators of the infrared and optical wavelength range. The linac injector (Fig. 1) is aimed to form short and intense electron bunches. It consists of an electron gun, an accelerator tube, a subharmonic prebuncher and a standing-wave acceleration section (buncher). The injection scheme is similar to that described by Tomimasu *et al.* (1998).

The electron beam is preliminarily formatted by the gun, with a grid electrode, which generates short bunches of length 0.5 ns and a bunched beam current up to 4 A. The bunch length at the gun exit is given by the formula

Table 1
Summary of FEL radiation properties.

G1–G4 refer to the FEL oscillators. FIR stands for the far-infrared coherent source.

	FIR	G1	G2	G3	G4
Radiation wavelength (μm)	150–1000	20–150	5–30	1–6	0.15–1.2
Peak output power (MW)	10–100	1–5	1–5	3–15	10–20
Micropulse energy (μJ)	500	50–200	25–100	25–100	50–100
Micropulse duration, FWHM (ps)	5–10	10–30	10	10	3–5
Spectrum bandwidth, FWHM (%)		0.2–0.4	0.6	0.6	0.6
Average output power (W)	10–50	0.2–1			
Micropulse repetition rate (MHz)	19.8/39.7/59.5				
Macropulse duration (μs)	5–10				
Repetition rate (Hz)	1–100				

Table 2
Undulator specifications for the DELSY project.

	U1	U2	U3	U4
Type	Hybrid, planar			
Period (cm)	8	5.5	4	3.2
Peak magnetic field (T)	0.8–0.26	0.95–0.25	1.0–2.5	0.8–2.0
Gap (mm)	2.5–5.0	1.0–3.5	1.0–2.5	0.8–2.0
Number of periods	35	40	60	80
Total length (cm)	280	220	240	256

Table 3
Electron beam parameters list for the DELSY project.

	FEL1	FEL2	FEL3	FEL4
Energy (MeV)	30–60	30–70	50–110	120–280
Bunch charge (nC)	1			
Peak current (A)	50–70	150–250		
Bunch length, r.m.s. (mm)	2.4	0.5–0.8		
Normalized emittance, r.m.s. (mm mrad)	30			
Energy spread, r.m.s. (keV)	150	450–750		

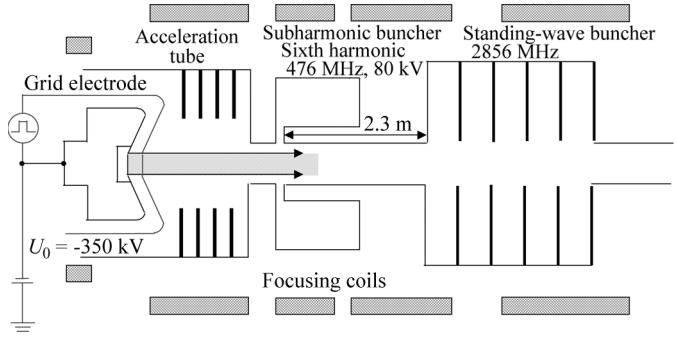

Figure 1
Injector scheme.

† Presented at the 'XIV Russian Synchrotron Radiation Conference SR2002', held at Novosibirsk, Russia, on 15–19 July 2002.

$$l_{\rm gun} = \beta_{\rm gun} c \tau_0,$$

where $\beta_{\rm gun}$ is the electron velocity, τ_0 is the micropulse duration and c is the speed of light. Then electrons enter the subharmonic buncher (SHB) where they gain or lose energy depending on the RF voltage phase,

$$\Delta\varepsilon = \pm eV_0 \sin \Omega t, \qquad \Omega = 2\pi f.$$

Here V_0 and f (= 476 MHz) are the amplitude and frequency of the SHB RF voltage. The SHB voltage is phased in such a way that the electrons of the bunch head lose energy, while the tail electrons gain energy. As a result, the bunch shrinks in the first drift section. The SHB is a quarter-wavelength cavity with a gap of 1 cm and a voltage amplitude of 100 kV. After the SHB the electrons pass through the 2.3 m-long drift section where the bunch length reduces to 5 mm (Fig. 2).

The drift section is followed by the standing-wave acceleration section (bunch compressor, BC), which has a length of 4λ at a frequency of 2856 MHz. If the acceleration field amplitude is 25 MV m^{-1} the bunch length decreases in the BC to 2–3 mm and the peak current reaches a value of 100 A (Fig. 3*a*, Table 4). At 40 MV m^{-1} one can obtain 1–2 mm and 500 A, respectively (Fig. 3*b*, Table 4). Another critical requirement is the formation of the bunch with a small emittance. For this purpose we have chosen a formation scheme with a longitudinal magnetic field and a gun cathode placed outside the field. The field value is defined by the well known formula for 'the Brillouin beam',

$$B_s\,[\mathrm{T}] = 3.69 \times 10^{-5} \left(I\,[\mathrm{A}]/\beta\gamma\right)^{1/2} / r\,[\mathrm{m}],$$

where I is the beam current, r is the bunch radius and γ is the Lorentz factor. The proper field distribution (Fig. 4) and coil with opposite field direction at the injector exit allow the formation of a beam with the required emittance. The evolution of the beam parameters from the gun to the first section exit (Fig. 5) shows an efficient bunch formation. Simulation of the electron beam dynamics in the injector was performed using the computer code *ASTRA* (http://www.desy.de/~mpyflo/Astra_dokumentation/); the injector design is in progress.

2. Phase II: storage ring

2.1. Lattice and basic parameters

Phase II will be accomplished with the commissioning of the storage ring. The DELSY storage ring is designed to use upgraded equipment from the AmPS storage ring. The optics of the DELSY storage ring are characterized by its twofold symmetry. Each quadrant consists of the MBA (multi-bend achromat) structure: two halves of the straight sections and two periodic cells (Titkova, Beloshitsky *et al.*, 2000; Beloshitsky *et al.*, 2001). The main machine parameters are given in Table 5. The beta functions in a very strong wiggler are β_x = 1.05 m and β_y = 2.80 m (Fig. 6); in the undulator they were taken to be β_x = 14.55 m and β_y = 0.98 m (Fig. 7). The measured multipole

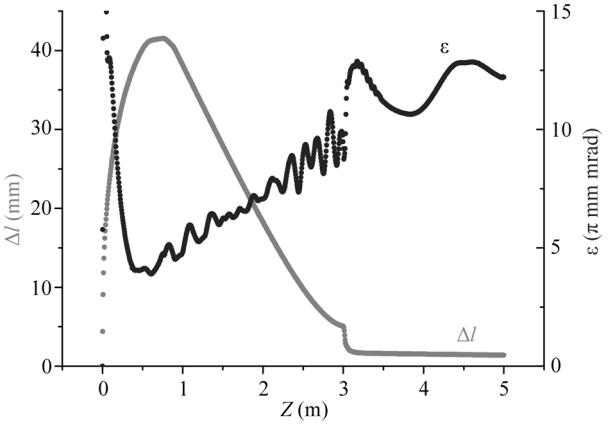

Figure 2
Bunch length and emittance variation along the injector. E = 40 MV m^{-1}, Q = 1.2 nC, Z is the distance from the gun exit.

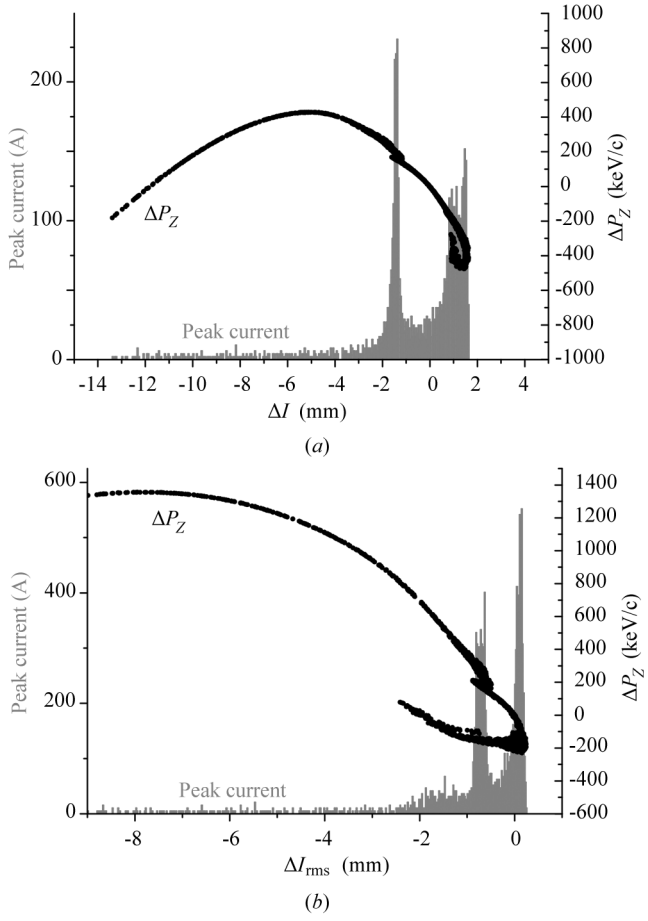

Figure 3
Peak current and energy spread at an acceleration field of (*a*) 25 MV m^{-1} (ε = 5.1 MeV, Q = 1.2 nC, Z = 4 m) and (*b*) 40 MV m^{-1} (ε = 8 MeV, Q = 1.2 nC, Z = 4 m).

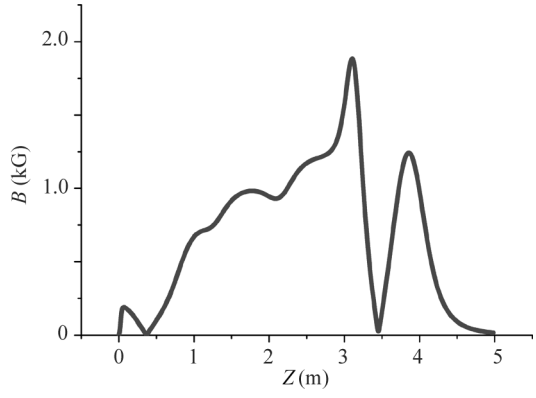

Figure 4
Magnetic field distribution in the injector.

Table 4
Electron beam parameters at the BC exit.

	Acceleration field amplitude	
	25 MV m^{-1}	40 MV m^{-1}
Energy (MeV)	5	8
Bunch charge (nC)	1.2	1.2
Peak current (A)	100–150	300–500
Bunch length, r.m.s. (mm)	2–3	1–2
Normalized emittance (mm mrad)	10–20	10–20
Energy spread, r.m.s. (keV)	200	400

components of the 10 T wiggler (N. A. Mezentsev, private communication) were used for the linear optics and dynamic aperture calculations with the wiggler on. After compensating for the influence of the wiggler, the deviation of the beta functions for the machine with the wiggler on and off is less than 7%; the emittance increased to 21.3 nm. The effect of the undulator on the machine optics is much smaller. The deviation of the beta functions for the machine with the undulator on is less than 1%; the emittance decreased to 11.14 nm.

2.2. Synchrotron radiation spectra

The synchrotron radiation from the dipole magnets of DELSY with a maximum brilliance of 3.9×10^{14} photons s^{-1} mm^{-2} mrad^{-2} (0.1% bandwidth)$^{-1}$ (Beloshitsky *et al.*, 2001) has rather a high intensity in both the ultraviolet and infrared regions. Eight beamlines are planned to be constructed for the synchrotron radiation from the bending magnets. For a beam current of 300 mA the maximum brilliance from the 10 T wiggler is 1.6×10^{15} photons s^{-1} mm^{-2} mrad^{-2} (0.1% bandwidth)$^{-1}$. Six beamlines will be constructed for the synchrotron radiation from the wiggler. The synchrotron radiation from the undulator with a maximum brilliance of 2.1×10^{19} photons s^{-1} mm^{-2} mrad^{-2} (0.1% bandwidth)$^{-1}$ can be used for VUV luminescence of crystals and pumping of VUV lasers, for metrology and photometry. For this purpose two beamlines will be constructed.

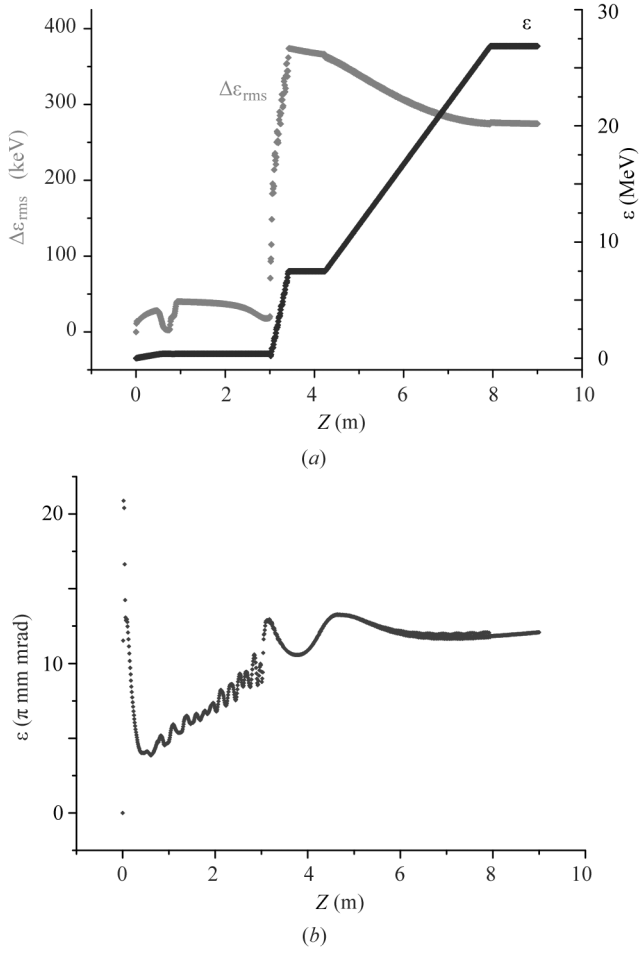

Figure 5
Energy spread and (*a*) energy and (*b*) emittance variation along the injector. $E = 40$ MV m^{-1}, $Q = 1.2$ nC.

Table 5
Main parameters of the DELSY ring.

Full energy (GeV)	1.2
Injection energy (GeV)	0.8
Circumference (m)	136.04
Bending radius (m)	3.3
Betatron tunes, h/v	9.44/3.42
Momentum compaction factor	5.03×10^{-3}
Natural chromaticity, h/v	−22.2/−12.6
Injection current (mA)	10
Stored electron current (mA)	300
Horizontal emittance (nm)	11.4
RF frequency (MHz)	476
Harmonic number	216
Energy loss per turn (keV)	55.7

2.3. Dynamic aperture and closed-orbit correction

The dynamic aperture calculated using the *MAD* computer code (Grote & Iselin, 1996) is $77\sigma_x$ and $90\sigma_y$ (without influence of the insertion devices). When the wiggler is on, the dynamic aperture decreases to $63\sigma_x$ and $86\sigma_y$; with the undulator on it is $68\sigma_x$ and $88\sigma_y$. In both cases the dynamic aperture is large enough to provide a good lifetime.

All misalignment and field errors were supposed to be Gaussian distributed with a cut-off at 3σ. The bending magnets have 1 mrad of misrotation along the longitudinal axis and 5×10^{-4} error fields; the quadrupoles have 200 μm of misalignment along the horizontal and

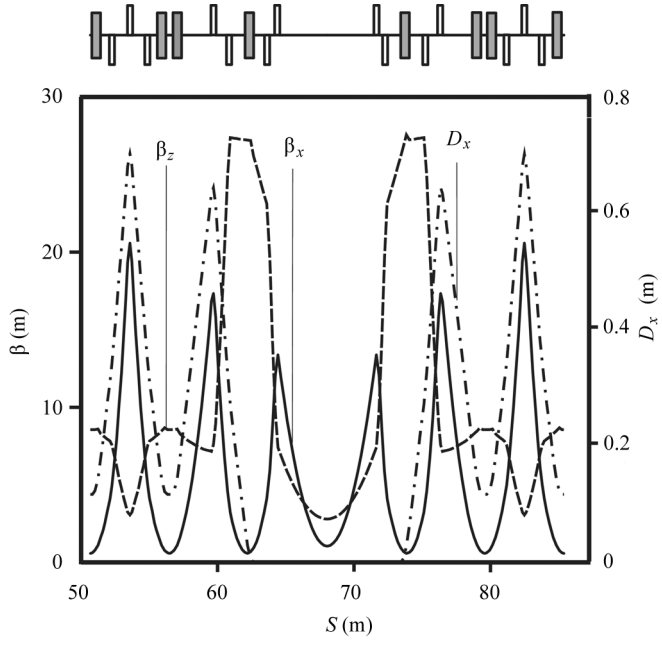

Figure 6
Lattice functions in the section with the very strong wiggler.

vertical axes. Two schemes for the position of the correctors have been studied (Beloshitsky *et al.*, 2001). Fifty machines have been studied. The maximum closed-orbit deviations (CODs) were found to be 15 mm and 26 mm for the horizontal and vertical planes, respectively. One of the machines was found to be unstable owing to the sum coupling resonance. After the orbit correction was applied (for the lattice with the insertion devices switched off), the maximum horizontal COD was 1.8 mm for the first scheme and 3 mm for the second scheme; the vertical COD was 0.99 mm for both schemes. The maximum horizontal corrector strength is 0.84 mrad in the first scheme and 0.74 mrad in the second scheme.

The dynamic aperture was calculated for two sets of errors, one with the maximum COD and the other with a typical COD. In the first scheme (40 correctors for the horizontal plane and 32 for the vertical plane) the dynamic aperture was found to be $59\sigma_x$ and $91\sigma_y$ for the variant with the maximum COD and $67\sigma_x$ and $83\sigma_y$ for the variant with the typical COD. In the second scheme (24 correctors for the horizontal plane and 32 for the vertical plane) the dynamic aperture was $58\sigma_x$ and $100\sigma_y$, $64\sigma_x$ and $96\sigma_y$, respectively. Thus, the dynamic aperture at the septum is 17 mm, which is high enough for effective injection. With the correctors turned on, the emittance change is insignificant. When the wiggler is on, the dynamic aperture is $53\sigma_x$ and $87\sigma_y$ for the error set with the maximum COD.

3. Development of the modified dipole magnet for the electron storage ring DELSY

The dipole magnets of the AmPS storage ring allowed the level of the magnetic field to be $\sim$1 T at the maximal coil excitation current 330 A (the pole gap was 45 mm). A test magnet was designed and made to choose the necessary pole geometry for the modified dipole magnet. Modification of the pole consisted of reducing the pole gap to 38 mm and changing the pole shape with the purpose of additional concentration of the magnetic flux. A magnetic measurement stand was assembled and adjusted to measure and shape the magnetic field for the DELSY dipole magnet. Magnetic measurements included measurement of the full field map by the Hall probe and measurement of a change in the longitudinal magnetic field integral by the induction method. The magnetization curve for the modified magnet in comparison with the appropriate curve for the AmPS dipole magnet is given in Fig. 8. Fig. 9 shows the normalized dependencies from the cross coordinate of change of the longitudinal magnetic field integral for the dipole magnet at the minimal and maximal working values of the magnet coil excitation current.

The required relative uniformity of the magnetic field integral, $\pm 5 \times 10^{-4}$, is achieved in the horizontal working aperture $\pm$30–40 mm. In order to shape the magnetic field of the dipole magnet of DELSY, computer calculations using the two-dimensional code *SUPERFISH* (Billen & Young, 1997) and the three-dimensional code *RADIA* (Chavanne *et al.*, 2001) were used.

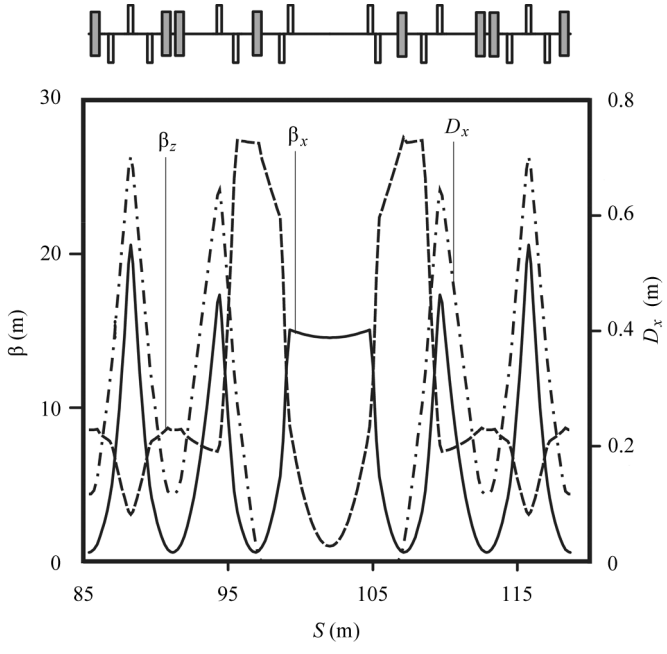

Figure 7
Lattice functions in the section with the undulator.

4. Conclusions

The modified injector linac will generate short and intense electron bunches which can be used for FEL pumping. A few types of FELs covering a wide spectrum range are planned to be constructed. Based on the magnetic elements of the AmPS, the DELSY storage ring will be a third-generation synchrotron source. The machine optics make it possible to install at least one very strong wiggler with a magnetic field of 10 T and one undulator. The dynamic aperture is large enough

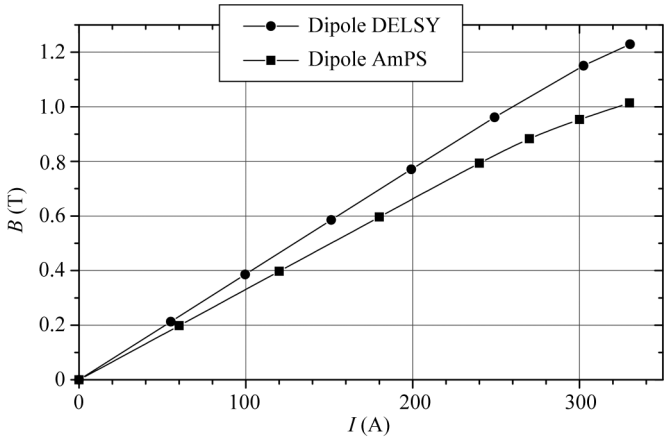

Figure 8
Magnetization curve for the modified magnet in comparison with the appropriate curve for the AmPS dipole.

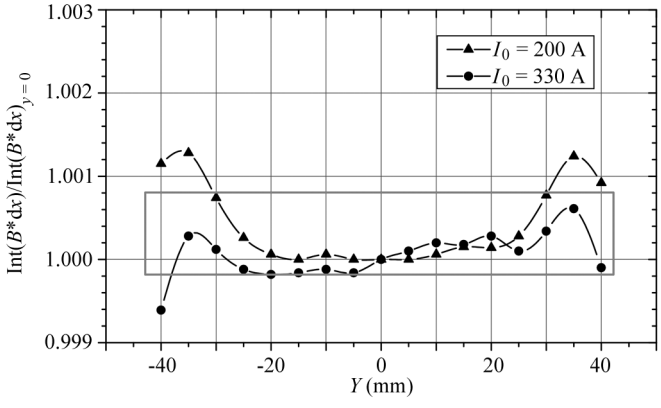

Figure 9
Normalized dependencies from the cross coordinate of charge of the longitudinal magnetic field integral for the dipole magnet at the minimal and maximal working values of the magnet coil excitation current.

to provide effective injection and good lifetime during operation with the insertion devices turned on. The scheme of the closed-orbit correction allows the correctors from the AmPS to be used.

References

Arkhipov, V. A., Antropov, V. K., Balalykin, N. I., Beloshitskya, P. F., Boer-Rookhuizenb, H., Brovkoa, O. I., Butenkoa, A. B., Fedorenkoa, S. B., Ivanova, I. N., Heineb, E., Heubersb, W. P. J., Kaanb, A. P., Kadyshevskya, V. G., Kalinichenkoa, V. V., Kobetsa, V. V., Krasavina, E. A., Kroesb, F. B., Kuijerb, L. H., Kulipanovc, G. N., Laanb, J. B. V. D., Langelaarb, J., Levichevc, E. B., Louwrierb, P. W. F., Luijckxb, G., Maasb, R., Meshkov, I. N., Mezentsevc, N. A., van Middelkoopb, G., Minashkina, V., Morozova, N. A., Noomenb, J. G., Polyakova, Yu. A., Russakovicha, N. A., Sidorina, A. O., Sidorova, A. I., Sidorova, G. I., Sissakyana, A. N., Shakuna, N. G., Shatunovc, E. M., Shvetsa, V. A., Skrinskyc, A. N., Smirnova, V. I., Sumbaeva, A. P., Speltb, J. B., Syresina, E. M., Titkovaa, I. V., Tyutyunnikova, S. I., Ushakovc, V. A., Voblyc, P. D., Vodopyanova, A. S. & Yurkov, M. V. (2001). *Nucl. Instrum. Methods*, A**470**, 1–6.

Arkhipov, V. A., Antropov, V. K., Balalykin, N. I., Beloshitskya, P. F., Brovkoa, O. I., Butenkoa, A. B., Fedorenkoa, S. B., Ivanova, I. N., Kadyshevskya, V. G., Kalinichenkoa, V. V., Kobetsa, V. V., Krasavina, E. A., Meshkova, I. N., Minashkina, V., Morozova, N. A., Polyakova, Yu. A., Russakovicha, N. A., Sidorina, A. O., Sidorova, A. I., Sidorova, G. I., Sissakyana, A. N., Shakuna, N. G., Shvetsa, V. A., Smirnova, V. I., Sumbaeva, A. P., Syresina, E. M., Titkovaa, I. V., Tyutyunnikova, S. I., Vodopyanova, A. S., Yurkova, M. V., Boer-Rookhuizenb, H., Heineb, E., Heubersb, W. P. J., Kaanb, A. P., Kroesb, F. B., Kuijerb, L. H., Laanb, J. B. V. D., Langelaarb, J., Louwrierb, P. W. F., Luijckxb, G., Maasb, R., van Middelkoopb, G., Noomenb, J. G., Speltb, J. B., Kulipanovc, G. N., Levichevc, E. B., Mezentsevc, N. A., Shatunovc, E. M., Skrinskyc, A. N., Ushakovc, V. A., Voblyc, P. D., Kolobanovd, V. N. & Mikhailin, V. V. (2001). *Nucl. Instrum. Methods*, A**467**, 59–62.

Beloshitsky, P., Meshkov, I. & Titkova, I. (2001). *Proceedings of the 2001 Particle Accelerator Conference (PAC 2001)*, Vol. 4, p. 2821. Piscataway, NJ: IEEE.

Billen, J. H. & Young, L. M. (1997). *POISSON SUPERFISH.* Report LA-UR-96–1834. Los Alamos National Laboratory, Los Alamos, NM, USA.

Chavanne, J., Chubar, O. & Elleaume, P. (2001). *RADIA. A Three-Dimensional Magnetostatic Computer Code.* ESRF, Grenoble, France.

Grote, H. & Iselin, F. C. (1996). *MAD User's Reference Manual.* Version 8.19. CERN SL/90–13 (AP) (Rev. 5). CERN, Geneva, Switzerland.

Saldin, E. L., Schneidmiller, E. A. & Yurkov, M. V. (2000). *The Physics of the Free-Electron Lasers.* Berlin: Springer-Verlag.

Titkova, I. V., Arkhipov, V. A., Antropov, V. K., Balalykin, N. I., Beloshitsky, P. F., Brovko, O. I., Butenko, A. B., Fedorenko, S. B., Ivanov, I. N., Kadyshevsky, V. G., Kalinichenko, V. V., Kobets, V. V., Krasavin, E. A., Meshkov, I. N., Minashkin, V., Morozov, N. A., Polyakov, Yu. A., Russakovich, N. A., Sidorin, A. O., Sidorov, A. I., Sidorov, G. I., Sissakyan, A. N., Shakun, N. G., Shvets, V. A., Smirnov, V. I., Sumbaev, A. P. , Syresin, E. M., Tyutyunnikov, S. I., Vodopyanov, A. S., Yurkov, M. V., Boer-Rookhuizen, H., Heine, E., Heubers, W. P. J., Kaan, A. P., Kroes, F. B., Kuijer, L. H., Laan, J. B. V. D., Langelaar, J., Louwrier, P. W. F., Luijckx, G., Maas, R., van Middelkoop, G., Noomen, J. G., Spelt, J. B., Kulipanov, G. N., Levichev, E. B., Mezentsev, N. A., Shatunov, E. M., Skrinsky, A. N., Ushakov, V. A. & Vobly, P. D. (2000). *Proceedings of the Seventh European Particle Accelerator Conference (EPAC 2000)*, pp. 702–704, 26–30 June 2000, Vienna, Austria.

Titkova, I. V., Beloshitsky, P. F., Meshkov, I. N. & Syresin, E. M. (2000). *Proceedings of the Seventh European Particle Accelerator Conference (EPAC 2000)*, pp. 708–710, 26–30 June 2000, Vienna, Austria.

Tomimasu, T., Mori, Y., Oshita, E., Okuma, S., Nishihara, S. & Takii, T. (1998). *Nucl. Instrum. Methods*, A**407**, 370–373.

 Received 25 January 2003 • Accepted 19 May 2003